Korea-Australia Rheology Journal, Vol.26, No.1, pp.63-71 (February 2014) www.springer.com/13367
DOI: 10.1007/s13367-014-0007-3

Fabrication of porous polymer microparticles with tunable pore size and density through the combination of phase separation and emulsion-solvent evaporation approach

Shanqin Liu[1,§], Mingle Cai[1,§], Renhua Deng[1], Jianying Wang[1], Ruijing Liang[1] and Jintao Zhu[1,2,*]
[1]*Key Laboratory for Large-Format Battery Materials and System of Ministry of Education, School of Chemistry and Chemical Engineering, Huazhong University of Science and Technology (HUST), Wuhan, 430074, P. R. China*
[2] *National Engineering Center for Nanomedicine, HUST, Wuhan, 430074, P. R. China*

(Received October 29, 2013; final revision received December 26, 2013; accepted January 6, 2014)

A facile and versatile route to prepare porous polymer microparticles with tunable pore size and density through the combination of phase separation and emulsion-solvent evaporation method is demonstrated. When volatile organic solvent (*e.g.*, chloroform) diffuses through the aqueous phase containing poly(vinyl alcohol) (PVA) and evaporates, *n*-hexadecane (HD) and polystyrene (PS) in oil-in-water emulsion droplets occur to phase separate due to the incompatibility between PS and HD, ultimately yielding microparticles with porous structures. Interestingly, density of the pores (pore number) on the shell of microparticles can be tailored from one to hundreds by simply varying the HD concentration and/or the rate of solvent evaporation. Moreover, this versatile approach for preparing porous microparticles with tunable pore size and density can be applied to other types of hydrophobic polymers, organic solvents, and alkanes, which will find potential applications in the fields of pharmaceutical, catalyst carrier, separation, and diagnostics.

Keywords: porous microparticles, emulsion droplets, solvent evaporation, phase separation, pore size

1. Introduction

Recently, porous polymer microparticles have received increasing interest because of their high surface area, relatively low density and good permeability compared to nonporous polymer microparticles, potentially useful in the fields of catalysis (Ding *et al*., 2011), separation (Slater *et al.*, 2006), solid phase organic and peptide synthesis (Hudson *et al.*, 1999), ion-exchange (Rao *et al.*, 2004), gas storage (Wood *et al.*, 2008; Li *et al*., 2010), drug storage and delivery (Chung *et al.*, 2006), and diagnostics (Bae *et al*., 2009). Pore size and density play key roles in determining the properties of the porous polymer particles, including drug encapsulation efficiency and release kinetics, cellular uptake, catalysis activities and efficiency (Klose *et al*., 2006; Kim *et al*., 2010), among others. Thus, considerable efforts have been made to precisely control these physical parameters of the polymer particles. It is well known that porous microparticles can be classified as macro- (>50 nm), meso- (50-2 nm) and microporous (<2 nm) materials depending on the size of the pores (Sing *et al.*, 1985). Usually, the formation of pores in the polymer particles is a process of phase separation either in suspension polymerization or swelling and polymerization. The control variables of pore size mainly include the effect of the cross-linking monomer and porogen, the reaction temperature, swelling ratio of seed polymer, solvent evaporation rate, and others (Svec *et al*., 1996; Durie *et al*., 2002; Jose *et al*., 2005).

To date, many approaches for the fabrication of porous polymer particles have been developed, including seeded emulsion, suspension or dispersion polymerization (Okubo *et al.*, 2005; Kong *et al.*, 2008), microfluidics-assisted route (Gokmen *et al.*, 2009; Gong *et al.*, 2009; Watanabe *et al.*, 2011), emulsion-solvent evaporation method (Yabu *et al.*, 2005; Shi *et al.*, 2011; Watanabe *et al.*, 2011; Deng *et al.*, 2012; Jang *et al.*, 2012) and internal phase-separation approach (Loxley *et al*., 1998; Yow *et al*., 2008; Kim *et al.*, 2010; Tanaka *et al.*, 2010). Although these approaches demonstrate their own advantages in generating porous polymer particles at different scales, their limitations are also obvious (Gokmen *et al.*, 2012; Wu *et al.*, 2012). For example, polymerization-based approaches, including seeded emulsion, suspension or dispersion polymerization, can be conducted to generate porous particles with porogen under the effect of emulsifier and the aid of mechanical stirring. Monomers are usually dispersed in water and the polymerizations are triggered by the initiator. This polymerization approach is simple to conduct but difficult to regulate the porous size and density. Although progresses have been achieved for the preparation of porous polymer microparticles in recent years (Gokmen *et al.*, 2012; Wu *et al.*, 2012; Zou *et al.*, 2013), it is still a challenge to generate porous polymer microparticles with tunable pore size and density.

*Corresponding author: jtzhu@mail.hust.edu.cn
§These authors contributed equally to this work

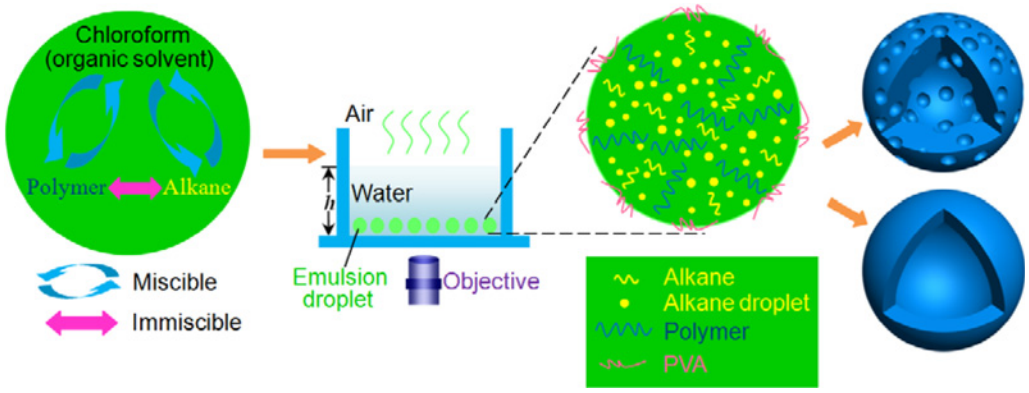

Scheme 1. (Color online) Schematic illustration of the formation of porous polymer microparticles. The organic phase consisted of polymer and alkane (*e.g.*, *n*-hexadecane) in chloroform and aqueous phase consisted of 5 mg/mL poly(vinyl alcohol) (PVA) to stabilize the emulsion droplets against coalescence. After shaking the two phases vigorously, small emulsion droplets were formed and the emulsions were then transferred to a round designed device for adjusting solvent evaporation rate by varying the water layer height (*h*). With the evaporation of chloroform, microparticles with pores or microcapsules were generated owing to the incompatibility between the polymer and alkane.

Herein, we introduce a simple and effective method to fabricate macroporous polymer microparticles with tunable pore size and density based on the combination of phase separation and emulsion-solvent evaporation route. Solvent evaporation rate was controlled by varying the water layer height (*h*) in the evaporation device. Emulsion droplets containing polymer (*e.g.*, polystyrene (PS)) and nonsolvent (*e.g.*, *n*-hexadecane (HD)), which acts as a porogen dissolved in a volatile solvent (*e.g.*, chloroform), are generated by hand shaking vigorously using poly(vinyl alcohol) (PVA) as an emulsifier. After complete evaporation of the volatile solvent, porous polymer microparticles can be readily prepared through phase separation induced by the incompatibility of HD and PS. More importantly, the pore density and size can be easily tailored by adjusting HD concentration (C_{HD}) and/or the solvent evaporation rate. Furthermore, this facile method can be applied to a variety of polymers, alkanes, organic solvents, and so forth.

2. Experimental Section

2.1. Materials

Polystyrene ($PS_{2.8k}$, we refer $PS_{2.8k}$ as PS with M_n=2.8k, PDI=1.09; PS_{21k}, PDI=1.04; PS_{876k}, PDI=1.19), poly(methyl methacrylate) ($PMMA_{24k}$, PDI=1.25), PS-*b*-poly(methyl methacrylate) (PS_{25k}-*b*-$PMMA_{26k}$, PDI=1.06), polycaprolactone (PCL_{20k}, PDI=1.25), and poly(DL-lactic acid) (PLA_{50k}, PDI=1.20) were all purchased from Polymer Source. Inc., Canada. Nile red (purity >98%) and poly(vinyl alcohol) (PVA, M_w=13-23k, 87-89% hydrolyzed) were purchased from Sigma-Aldrich. *n*-hexadecane (HD) and chloroform were purchased from Shanghai Reagents Co., China. All of the materials were used without further purification.

2.2. Sample preparation

10 mg/mL polymer, 0.001 mg/mL Nile red and HD with varied concentration were dissolved in chloroform, which was then emulsified with aqueous solution containing 5 mg/mL PVA through simply shaking by hand. Chloroform was allowed to evaporate by leaving the emulsion in a designed round evaporation device with an inner diameter of 2.2 cm (see Scheme 1) at room temperature (~25°C). Depending on the height of water layer (*h*) in the device, evaporation process of the organic solvent would last tens of minutes to hours. After organic solvent evaporated completely, porous polymer microparticles formed and were collected by centrifugation for 15 min at 6000 rpm. The precipitated microparticles were then washed with deionized water three times to remove partial PVA and residual chloroform.

2.3. Characterization

2.3.1. Optical microscope

Real-time structural evolution of the shrinking emulsion droplets containing PS and HD was monitored using Olympus IX71 inverted optical microscope in the bright-field mode.

2.3.2. Confocal laser scanning microscope (CLSM)

The suspension of polymer microparticles was examined with a Fluoview FV1000 confocal laser scanning microscope equipped with a 1 mW helium-neon

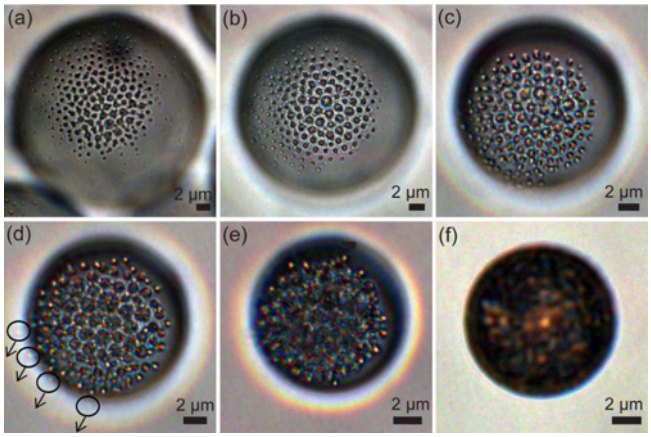

Fig. 1. (Color online) Optical microscopy images showed the evolution of the same emulsion droplet containing 10 mg/mL PS_{21k} and 2 mg/mL HD during chloroform removal at h=0.75 mm. The time elapse for the images was (a) 5 sec, (b) 12 min, (c) 16 min, (d) 19 min, (e) 20 min, and (f) 30 min. We note that polymer and HD can dissolve well in chloroform in our experiment, and no HD droplets were formed before and right after emulsification. When we perform the optical microscopy investigation by dropping the emulsion on the glass slides (~ 5 sec), tiny droplets can be seen within the emulsion droplet (Fig. 1a). Control experiment indicates that no tiny droplets were observed for the emulsions without the addition of HD. Thus, the tiny droplets within the emulsion can be ascribed to the HD phase due to the phase separation between HD and the polymer during solvent evaporation.

laser. The red fluorescence signal, originated from Nile red, was observed with a long-pass 590 nm emission filter under a 515 nm laser illumination. The pinhole diameter was set at 71 mm. Stacks of images were collected every 0.5 μm along the z-axis.

2.3.3. Scanning electron microscope (SEM)

SEM was carried out on a Sirion 200 scanning electron microscope at an accelerating voltage of 10 kV. To prepare samples for SEM, a drop of the centrifugal microparticles dispersion was dropped on a clean silicon wafer, and water was allowed to evaporate. Then, the samples were coated with a thin layer of gold.

2.3.4. Brunauer-Emmett-Teller (BET)

BET specific surface area, N_2 adsorption isotherms (77.2 K), and pore size distribution of the polymer microparticles were measured by the BET method using a Micrometrics ASAP 2020 M surface area and porosity analyzer. The microparticles suspension was centrifuged at 5000 rpm and allowed to dry at room temperature under vacuum until a constant weight was obtained. Before analysis, the samples were degassed at 50°C for 8 h under vacuum (10^{-5} bar).

3. Results and Discussion

3.1. Porous microparticles generation through emulsion-solvent evaporation

In a typical experiment, PS and HD were first dissolved in chloroform which was a good solvent for both components, as shown in scheme 1. The solution was then emulsified with 5 mg/mL PVA aqueous solution through vigorously shaking by hand. Emulsion droplets with initial size of ~30-70 μm were thus generated. Afterwards, the emulsions were collected into a designed evaporation device (Scheme 1) and chloroform was allowed to remove by diffusing through the aqueous layer and evaporating into the surrounding air at ambient temperature (25°C). The rate of solvent evaporation was controlled by tailoring the height of water layer (h) (Liu *et al.*, 2012; Wang *et al.*, 2012).

The evolution process of an emulsion droplet during solvent evaporation was shown in Fig. 1. As the chloroform evaporates, tiny HD droplets within the emulsion droplet would appear and coalesce slowly into small HD droplets. The formed small HD droplets inside the emulsion droplets will trigger the formation of small holes in the resulting microparticles, while small HD droplets at the interface would depart from the emulsion droplet (Fig. 1d) and form plenty of pores on the shell of microparticles (Fig. 1f). The separated HD droplets from the emulsion droplets could be stabilized by the PVA in the aqueous solution. It was hard to observe the interior of microsphere with size of ~10 μm (Fig. 1f) from the optical microscopy image, but the hollow structure can be seen clearly for the cross-sectional SEM image in the inset of Fig. 2a. The reason for the formation of capsular structure can be ascribed to that the evaporation rate of chloroform in the center of emulsion droplet was slower than that at the edge. The small HD droplets in the center had enough time to coalesce to form a big HD droplet, resulting in the formation of a hollow core after complete removal of chloroform.

From Fig. 1 and 2, we can deduce that the formation mechanism of the porous polymer microparticles can be ascribed to phase separation between PS and HD during chloroform evaporation. We note that HD and the polymer can dissolve well in chloroform at first stage. With the evaporation of chloroform, concentration of the PS and HD will increase, leading to the aggregation of HD into tiny droplets due to the incompatibility of HD and PS, and the reduced solubility of HD in chloroform. Density of the HD droplets keeps similar as that of concentrated polymer solution in the droplets. Thus, the tiny HD droplets are uniformly distributed inside the polymer/chloroform drop, and porous structures are distributed homogeneously instead of spatially separated inside the polymer particles. Further removal of solvent will lead to the coalescence of the HD droplets and the

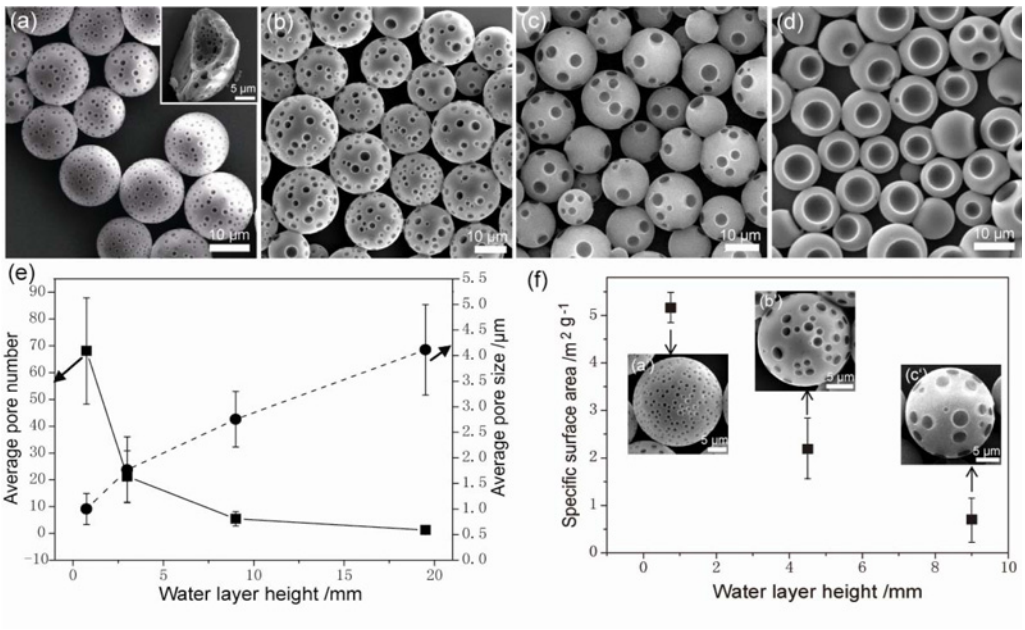

Fig. 2. (Color online) SEM images of porous polymer microparticles with different pore numbers were formed from emulsion droplets containing 2 mg/mL HD and 10 mg/mL PS_{21k} with varied *h*: (a, a') 0.75 mm, (b) 3 mm, (b') 4.5 mm, (c, c') 9 mm, (d) 19.5 mm. 5 mg/mL PVA was added to the aqueous phase to stabilize the emulsion droplets. (e) Plot shows the relationship between the water layer height *h* and average pore number (solid line)/average pore size (dashed line) of porous polymer microparticles in (a-d). Specifically, average pore number was obtained by counting only the visible side of the microparticles in SEM images; therefore, the pore number in the whole particle should be roughly two times as displayed in the plot, the same in Fig. 3. (f) The relationship between *h* and the specific surface area of PS porous microparticles in (a'-c').

increased viscosity of the polymer solution in the droplets, and porous structures could be trapped owing to the complete removal of chloroform and PS solidification. Finally, the HD droplets can be fixed both on the shell and the interior of polymer microparticles due to the high boiling point of HD. HD might evaporate from the microparticles under vacuum during the sample preparation for SEM investigation. In the previous work (Liu *et al.*, 2012), we used hexadecanol as a cosurfactant which displays amphiphilic character and can reduce the interfacial tension of oil/water further by adjusting the organization of surfactant molecules at the interface, ultimately leading to the interfacial instabilities of emulsion droplets. Compared with *n*-hexadecanol, *n*-hexadecane only has a hydrophobic alkyl chain which can only induce the phase separation and the generation of porous structure instead of triggering the interfacial instabilities. In this case, HD acts as a porogen for the formation of alkane domains in the PS matrix and ultimate pores after removal of the HD from the particles.

3.2. Porous microparticles with tailored pore size and number

The pore number and size of the porous microparticles can be tuned by simply adjusting the rate of solvent evaporation. Recently, we have successfully designed an evaporation device to control the rate of solvent evaporation by varying *h* (Liu *et al.*, 2012). With lower height for example *h*=0.75 mm, fast evaporation rate can be obtained, and phase separation between PS and HD close to the edge of emulsion droplet would occur quickly, resulting in porous microparticles with a large number of small pores. In this case, there is no enough time for HD coalescence into larger ones (Fig. 2a). While, in the center of emulsion droplet, small HD droplets will have enough time to coalesce and form a big HD droplet, leading to the formation of hollow core after complete removal of chloroform (see the inset of Fig. 2a). On the other hand, when the organic solvent evaporation rate is very slow (*h*=19.5 mm), the inner small HD droplets will have enough time to coalesce into a big one, finally resulting in the formation of polymer microcapsules with a single hole (Fig. 2d). Although several methods have been developed to generate porous particles, the method presented here represents a simple and effective route to tailor the pore size and density. When the height of water layer *h* was increased from 3 to 9 mm, the pore number of polymer microparticles decreased while the pore size of the polymer microparticles increased (Fig. 2b-c). The relationship between the water layer height *h* and average pore

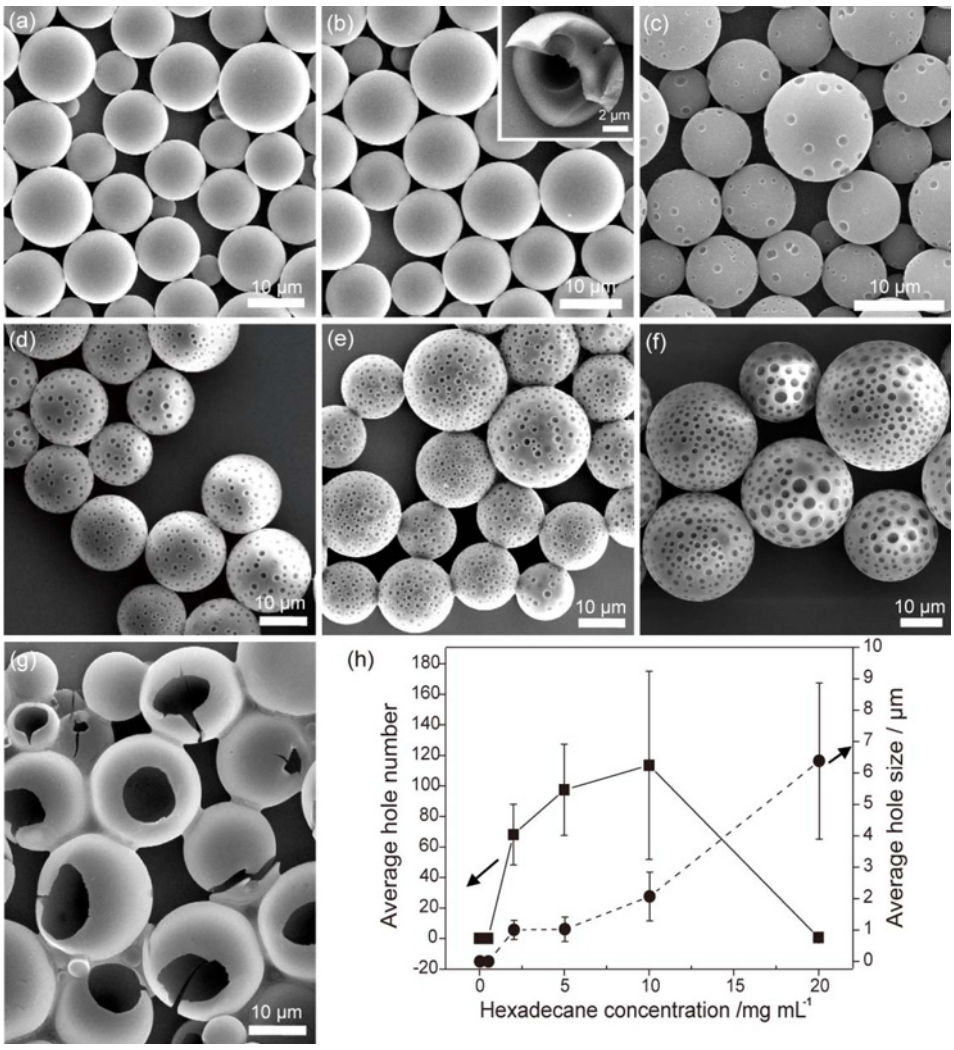

Fig. 3. (a-g) SEM images of PS microparticles formed from emulsion droplets containing 10 mg/mL PS_{21k} and different concentration of HD: (a) 0 mg/mL, (b) 0.5 mg/mL, (c) 1 mg/mL, (d) 2 mg/mL, (e) 5 mg/mL, (f) 10 mg/mL, (g) 20 mg/mL. Chloroform acts as an organic solvent while 5 mg/mL PVA was added to the aqueous phase to stabilize the emulsion droplets and *h* was set at 0.75 mm. (h) Plot shows the relationship between the HD concentration and average pore number (solid line)/average pore size (dashed line) for the PS microparticles in the (a-g).

number/average pore size is shown in Fig. 2e. Clearly, pore number decreases from ~ 68 to 1 whereas pore size increases from ~1.0 to 4.1 μm when increasing the height of water layer *h* from 0.75 to 19.5 mm. Fig. 2f illustrates the relationship between the water layer height *h* and the specific surface area of the PS porous microparticles determined by the BET measurement. The specific surface area of the PS porous microparticles decreases with the increase of *h* when C_{HD} is kept constant. The BET data further indicated that the pore number of the polymer microparticles can be controlled by using this method.

In addition, the concentration of HD (C_{HD}) also plays an important role in determining the pore number and size (Fig. 3). Our control experiment indicates that solid microparticles with smooth surface are obtained without the addition of HD (Fig. 3a). When the concentration of HD is 0.5 mg/mL, hollow microparticles with smooth surfaces are obtained after solidification. Due to the low concentration of HD, the time of forming HD droplets is increased under the same situation which has enough time for the tiny HD droplets to coalesce to large HD droplets and migrate to the center of emulsion droplets (Fig. 3b and inset). When increasing C_{HD} from 1 to 10 mg/mL, porous microparticles with increased pore number and reduced pore size are generated (Fig. 3c-f). However, when C_{HD} is increased up to 20 mg/mL, microparticles with a large single hole on the shell are generated (Fig. 3g) since high concentration of HD will easily induce the phase

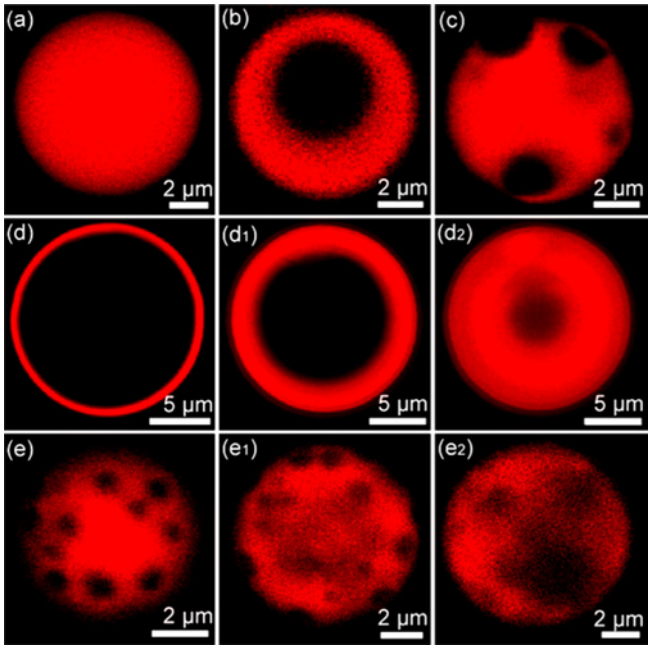

Fig. 4. (Color online) CLSM images of PS microparticles from emulsion droplets containing 10 mg/mL PS_{21k} and varied C_{HD} and h: (a) 0 mg/mL HD, h=3 mm, (b) 2 mg/mL HD, h=19.5 mm, (c) 2 mg/mL HD, h=9 mm, (d-d_2) 0.5 mg/mL HD, h=3 mm, (e-e_2) 2 mg/mL HD, h=3 mm. In (a-e_2) 0.1 wt % Nile red relative to the polymer was added to the initial polymer solution. (d-d_2) CLSM images of the same microparticle with different scanning depths: (d) 1.5 μm, (d_1) 5 μm, (d_2) 7.5 μm. (e-e_2) CLSM images of the same microparticle with different scanning depths: (e) 3.5 μm, (e_1) 5 μm, (e_2) 6.5 μm.

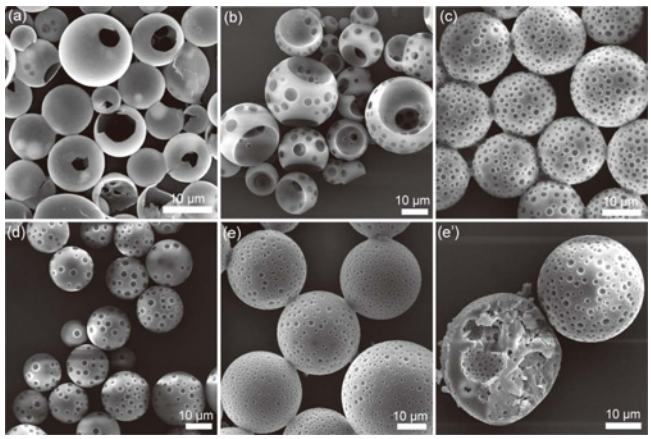

Fig. 5. SEM images of PS microparticles formed from emulsion droplets containing 5 mg/mL HD and varied concentration of PS_{21k}: (a) 1 mg/mL, (b) 5 mg/mL, (c) 10 mg/mL, (d) 20 mg/mL, (e) and (e') 40 mg/mL in chloroform as an organic phase. The water layer height h was set at 1.50 mm and 5 mg/mL PVA was added to the aqueous phase to stabilize the emulsion droplets. Clearly, phase separation occurs easily when the HD relative concentration was high (e.g., low polymer concentration). Microcapsules with a big hole (a) or (b) porous polymer microparticles with different sizes of pores were formed. With the increase of the PS concentration, many porous polymer microparticles with relatively uniform pores were obtained (c-d). When the PS concentration was increased up to 40 mg/mL, the pores in the surface of the porous polymer microparticles were shallow because the relative fraction of HD was very low in comparison with PS (e). (e') Cross-sectional SEM image of the microparticles in (e) which was cut by ultrathin knife. Clearly, there are a small hollow cavity and lots of pores on the surface of the cavity and the shell of the microsphere.

separation and coalescence of tiny HD droplets during chloroform evaporation. Fig. 3h shows the relationship between the HD concentration and average pore number/ average pore size.

CLSM images of PS microparticles in Fig. 4 confirmed that polymer microparticles with different internal morphologies can be created, including solid microparticles (Fig. 4a), porous microparticles (Fig. 4b, c) and microcapsules (Fig. 4d-d_2). Also, from the different depth of the CLSM image in Fig. 4e-e_2, we can conclude that small pores were distributed uniformly in the polymer particles. Moreover, the polymer microparticles have the capacity of encapsulation of hydrophobic species in the particles, demonstrating the potential applications of the porous particles in the field of drug delivery and release, catalysis, separation, and diagnostics. In addition, when changing initial concentration of PS (C_{PS}) under the same HD concentration, microcapsules with a hollow core or porous polymer microsphere with different sizes of pores can be obtained (Fig. 5), demonstrating more experimental variables of tuning the pore density and size for our technique.

All these results indicate that porous polymer microparticles with different pore number and size can thus be tuned simply by varying h, C_{PS} and/or C_{HD}.

3.3. Generality of the approach

To demonstrate the generality of our approach, investigations are performed by varying various experimental factors, including polymer type, polymer molecular weight, organic solvent, chain length of alkane, and the concentration of PVA.

Various types of polymers are used to prepare polymer microparticles, including PCL_{20k}, PLA_{50k}, $PMMA_{24k}$ and PS_{25k}-*b*-$PMMA_{26k}$ (see Fig. 6). Similar results were observed when these polymers were employed to fabricate porous microparticles, indicating the generality of our technique. Interestingly, this method can be applied to generate biodegradable polymer particles (*e.g.*, PCL and PLA) with tunable pore density and size by tuning the experimental parameters, which will expand the scope of applications in drug delivery and regenerative medicine.

Moreover, PS with varied molecular weights (Fig. 7)

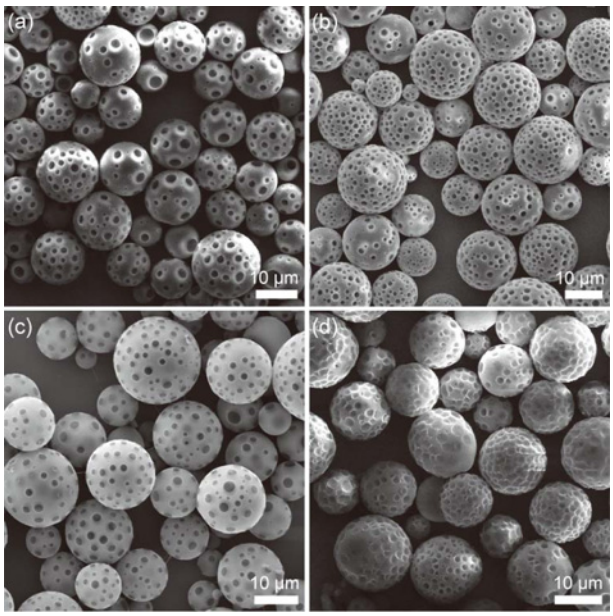

Fig. 6. SEM images of porous polymer microparticles from emulsion droplets containing 2 mg/mL HD and 10 mg/mL polymer: (a) PCL_{20k}, (b) PLA_{50k}, (c) $PMMA_{24k}$, (d) PS_{25k}-*b*-$PMMA_{26k}$. 5 mg/mL PVA was added to the aqueous phase to stabilize the emulsion droplets and *h* was set at 0.9 mm.

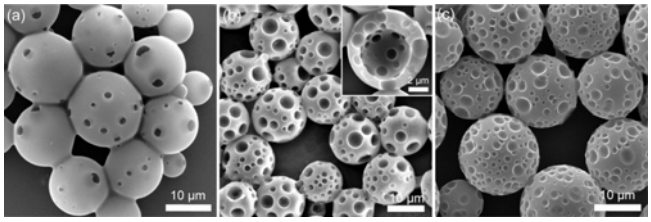

Fig. 7. SEM images of PS microparticles formed from emulsion droplets containing 5 mg/mL HD and 10 mg/mL PS with different molecular weight of: (a) $PS_{2.8k}$, (b) PS_{21k}, (c) PS_{876k}. 5 mg/mL PVA was added to the aqueous phase to stabilize the emulsion droplets and *h* was set at 3 mm. Inset in (b) is the cross-sectional SEM image of the porous particle.

and different organic solvents (Fig. 8) are employed to generate polymer microparticles by using the same procedure. In particular, the movement of PS chains in the emulsion droplets decreased for the increased viscosity and entanglement of PS during the evaporation of organic solvent with the increase of PS molecular weight. In this case, polymer with small molecular weight gives rise to microcapsules with several open holes on their surfaces (Fig. 7a) while polymer with high molecular weight will trigger the formation of polymer microparticles with dents on their surfaces (Fig. 7c). On the other hand, alkanes with varied chain length have been used to prepare polymer micoparticles by employing the same method. Fig. 9

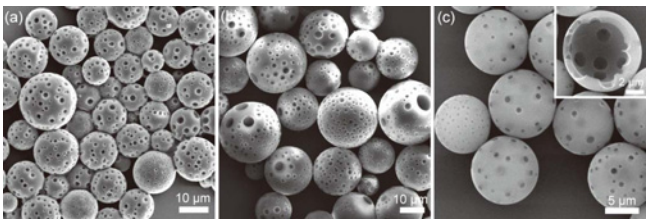

Fig. 8. SEM images of porous polymer microparticles formed from emulsion droplets containing 2 mg/mL HD and 10 mg/mL PS_{21k} in different commonly-used organic solvents: (a) carbon disulfide, (b) toluene, and (c) dichloromethane. Water layer height *h* was 0.9 mm and 5 mg/mL PVA was added to the aqueous phase to stabilize the emulsion droplets. Obviously, all of the organic solvents above could be used to generate porous polymer microparticles. Yet, microparticles with pores of high pore size dispersity were obtained when toluene was used. In this case, emulsion droplets would float on top of the water layer evaporated more freely and quickly because density of toluene was lower than water.

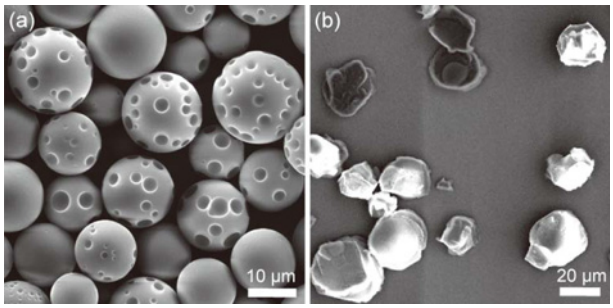

Fig. 9. SEM images of PS microparticles formed from emulsion droplets containing 10 mg/mL PS_{21k} in chloroform and 5 mg/mL alkanes: (a) *n*-hexane and (b) *n*-tetracosane. *h* was set at 0.9 mm and 5 mg/mL PVA was added to the aqueous phase to stabilize the emulsion droplets. Clearly, the type of alkanes plays an important role in the formation of porous microparticles.

showed that microparticles are produced when the chain length of alkane is in the range between 6 and 24. Our experiment indicates that *n*-hexane, which has a low boiling point (68.7°C), can evaporate easily and lead to the formation of polymer microparticles with non-uniform distribution of the pores (Fig. 9a). Yet, *n*-tetracosane, which has a very high boiling point (391°C), can not lead to the formation of porous microparticles (Fig. 9b). Presumably, medium chain alkane has the appropriate boiling point and solubility in the polymer solution to get enough time to trigger the phase separation. Therefore, the chain length of the alkanes from 6 to 20 is the desirable range for generating porous polymer microparticles. In addition, our result indicated that PVA concentration has no significant influence in the structure of the polymer particles (Fig. 10).

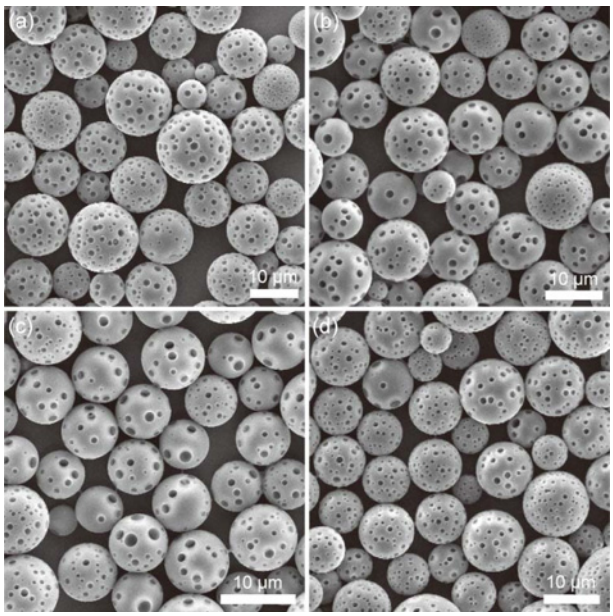

Fig. 10. SEM images of porous polymer microparticles formed from emulsion droplets containing 2 mg/mL HD and 10 mg/mL PS_{21k} in chloroform as the organic phase. Water layer height h was set at 0.9 mm. Aqueous solution containing PVA with various concentration was employed: (a) 1 mg/mL, (b) 3 mg/mL, (c) 5 mg/mL, and (d) 20 mg/mL. Clearly, PVA concentration plays limited role in the structure of porous polymer microparticles.

4. Conclusions

In summary, we have demonstrated a facile and effective approach to fabricate porous polymer microparticles with tunable pore size and number. Porous polymer microparticles are obtained by employing the emulsion-solvent evaporation method through phase separation induced by the incompatibility of HD and PS. Remarkably, pore size and density on the shell of microparticles can be easily tailored by varying the HD concentration and/or the rate of solvent evaporation. Moreover, this versatile approach can be extended to generate porous polymer microparticles for a broad range of hydrophobic polymers, alkanes, and organic solvents; and these porous polymer microparticles with tunable structures can be potentially useful in drug storage and delivery, catalyst carrier, gas storage, and so forth.

Acknowledgments

This work was supported by the funds from the National Basic Research Program of China (973 Program, 2012CB821500), National Natural Science Foundation of China (21004025 and 51103050). We also thank the HUST Analytical and Testing Center for allowing us to use its facilities.

References

Bae, S.E., J.S. Son, K. Park, and D.K. Han, 2009, Fabrication of covered porous PLGA microspheres using hydrogen peroxide for controlled drug delivery and regenerative medicine, *J. Control. Release* **133**, 37-43.

Chung, H.J., H.K. Kim, J.J. Yoon, and T.G. Park, 2006, Heparin immobilized porous PLGA microspheres for angiogenic growth factor delivery, *Pharm. Res.* **23**, 1835-1841.

Deng, R.H., S.Q. Liu, J.Y. Li, Y.G. Liao, J. Tao, and J.T. Zhu, 2012, Mesoporous block copolymer nanoparticles with tailored structures by hydrogen-bonding-assisted self-assembly, *Adv. Mater.* **24**, 1889-1893.

Ding, S.Y., J. Gao, Q. Wang, Y. Zhang, W.G. Song, C.Y. Su, and W. Wang, 2011, Construction of covalent organic framework for catalysis: Pd/COF-LZU1 in Suzuki-Miyaura coupling reaction, *J. Am. Chem. Soc*. **133**, 19816-19822.

Durie, S., K. Jerabek, C. Mason, and D.C. Sherrington, 2002, One-pot synthesis of branched poly(styrene divinylbenzene) suspension polymerized resins, *Macromolecules* **35**, 9665-9672.

Gokmen, M.T. and F.E. Du Prez, 2012, Porous polymer particles-A comprehensive guide to synthesis, characterization, functionalization and applications, *Prog. Polym. Sci.* **37**, 365-405.

Gokmen, M.T., W. Van Camp, P.J. Colver, S. Bon, and F.E. Du Prez, 2009, Fabrication of porous "clickable" polymer beads and rods through generation of high internal phase emulsion (HIPE) droplets in a simple microfluidic device, *Macromolecules* **42**, 9289-9294.

Gong, X., W. Wen, and P. Sheng, 2009, Microfluidic fabrication of porous polymer microspheres: dual reactions in single droplets, *Langmuir* **25**, 7072-7077.

Hudson, D., 1999, Matrix assisted synthetic transformations: A mosaic of diverse contributions. I. The pattern emerges, *J. Comb. Chem*. **1**, 333-360.

Jang, T.S., E.J. Lee, H.E. Kim, and Y.H. Koh, 2012, Hollow porous poly(epsilon-caprolactone) microspheres by emulsion solvent extraction, *Mater. Lett.* **72**, 157-159.

Jose, A.J., S. Ogawa, and M. Bradley, 2005, Tuning the pore size and surface area of monodisperse Poly(Methyl Acrylate) beads via parallel seeded polymerization, *Polymer* **46**, 2880-2888.

Kim, M.R., S. Lee, J.K. Park, and K.Y. Cho, 2010, Golf ball-shaped PLGA microparticles with internal pores fabricated by simple O/W emulsion, *Chem. Commun*. **46**, 7433-7435.

Klose, D., F. Siepmann, K. Elkharraz, S. Krenzlin, and J. Siepmann, 2006, How porosity and size affect the drug release mechanisms from PLGA-based microparticles, *Int. J. Pharm.* **314**, 198-206.

Kong, S.F., X.F. Wen, P.H. Pi, J. Cheng, and Z.R. Yang, 2008, Preparation and characterization of magnetic porous γ-Fe_2O_3/P(St-DVD-MAA) polymer microspheres, *Acta. Polym. Sin.* **2**, 168-173.

Li, B.Y., X. Huang, L.Y. Liang, and B.E. Tan, 2010, Synthesis of uniform microporous polymer nanoparticles and their applications for hydrogen storage, *J. Mater. Chem*. **20**, 7444-7450.

Liu, S.Q., R.H. Deng, W.K. Li, and J.T. Zhu, 2012, Polymer

microparticles with controllable surface textures generated through interfacial instabilities of emulsion droplets, *Adv. Funct. Mater*. **22**, 1692-1697.

Loxley, A. and B. Vincent, 1998, Preparation of poly (methylmethacrylate) microcapsules with liquid cores, *J. Colloid Interf. Sci.* **208**, 49-62.

Okubo, M., T. Fujibayashi, and A. Terada, 2005, Synthesis of micron-sized, monodisperse polymer particles of disc-like and polyhedral shapes by seeded dispersion polymerization, *Colloid Polym. Sci*. **283**, 793-798.

Rao, T.P., R.S. Praveen, and S. Daniel, 2004, Styrene-divinyl benzene copolymers: synthesis, characterization, and their role in inorganic trace analysis, *Crit. Rev. Anal. Chem*. **34**, 177-193.

Shi, X.D., L. Sun, and Z.H. Gan, 2011, Formation mechanism of solvent-induced porous PLA microspheres, *Acta. Polym. Sin.* **8**, 866-873.

Sing, K.S.W., D.H. Everett, R.A.W. Haul, L. Moscou, R.A. Pierotti, J. Rouquerol, and T. Siemieniewska, 1985, Reporting physisorption data for gas/solid systems with special reference to the determination of surface area and porosity, *Pure Appl. Chem*. **57**, 603-619.

Slater, M., M. Snauko, F. Svec, and J.M. Fréchet, 2006, "Click chemistry" in the preparation of porous polymer-based particulate stationary phases for μ-HPLC separation of peptides and proteins, *Anal. Chem*. **78**, 4969-4975.

Svec, F. and J.M. Fréchet, 1996, New designs of macroporous polymers and supports: from separation to biocatalysis, *Science* **273**, 205-211.

Tanaka, T., Y. Komatsu, T. Fujibayashi, H. Minami, and M. Okubo, 2010, A novel approach for preparation of micrometer-sized, monodisperse dimple and hemispherical polystyrene particles, *Langmuir* **26**, 3848-3853.

Wang, N.X., Y.G. Liao, R.H. Deng, S.Q. Liu, N. Cao, B.E. Tan, J.T. Zhu, and X.L. Xie, 2012, Polymer–inorganic hybrid microparticles with hierarchical structures formed by interfacial instabilities of emulsion droplets, *Soft Matter* **8**, 2697-2704.

Watanabe, T., T. Ono, and Y. Kimura, 2011, Continuous fabrication of monodisperse polylactide microspheres by droplet-to-particle technology using microfluidic emulsification and emulsion-solvent diffusion, *Soft Matter* **7**, 9894-9897.

Wood, C.D., B.E. Tan, A. Trewin, F. Su, M.J. Rosseinsky, D. Bradshaw, Y. Sun, L. Zhou, and A.I. Cooper, 2008, Microporous organic polymers for methane storage, *Adv. Mater.* **20**, 1916-1921.

Wu, D.C., F. Xu, B. Sun, R.W. Fu, H.K. He, and K. Matyjaszewski, 2012, Design and preparation of porous polymers, *Chem. Rev.* **112**, 3959-4015.

Yabu, H., T. Higuchi, K. Ijiro, and M. Shimomura, 2005, Spontaneous formation of polymer nanoparticles by good-solvent evaporation as a nonequilibrium process, *Chaos* **15**, 047505.

Yow, H.N., and A.F. Routh, 2008, Colloidal buckets formed via internal phase separation, *Soft Matter* **4**, 2080-2085.

Zou, S.W., H. Liu, Y. Yang, Z.J. Wei, and C.Y. Wang, 2013, Multihollow nanocomposite microspheres with tunable pore structures by templating Pickering double emulsions, *React. Funct. Polym.* **73**, 1231-1241.